NURETH14-391

FUEL ASSEMBLY SIMULATIONS USING LRGR-CFD AND CGCFD

F. Roelofs¹, V.R. Gopala¹, L. Chandra², M. Viellieber³, A. Class³

NRG, Petten, Netherlands

Currently working at IIT Rajasthan, India

KIT, Karlsruhe, Germany

roelofs@nrg.eu

Abstract

In addition to the traditional fuel assembly simulation approaches using system codes, subchannel codes or porous medium approaches, as well as detailed CFD simulations to analyze single sub channels, a Low Resolution Geometry Resolving (LRGR) CFD approach and a Coarse-Grid-CFD (CGCFD) approach is taken. Both methods are based on a low resolution mesh that allows the capture of large and medium scale flow features such as recirculation zones, which cannot be reproduced by the system codes, subchannel codes and porous media approaches.

The LRGR approach allows for instance fine-tuning the porous parameters which are important input for a porous medium approach. However, it should be noted that the prediction of detailed flow features such as secondary flows is not feasible. Using this approach, the consequences of flow blockages for detection possibilities and cladding temperatures can be discussed.

Within the Coarse-Grid CFD approach a subgrid model (SGM) accounts for sub grid volumetric forces which are derived from validated CFD simulations. The volumetric forces take account of the non resolved physics due to the coarse mesh. The CGCFD approach with SGM can be applied to simulate complete fuel assemblies or even complete cores capturing the unique features of the complex flow induced by the fuel assembly geometry and its spacers. In such a case, grids with a very low grid resolution are employed. The current paper discusses and presents both, the CGCFD and the LRGR approaches.

Introduction

The heart of every nuclear reactor is the core where the nuclear chain reaction takes place, heat is produced in the nuclear fuel and transported to a coolant. Almost all reactor cores consist of many fuel assemblies which in turn consist of a large number of fuel rods. For the design and safety analyses of such reactors, simulations of the heat transport within the core are essential. During the sixties, seventies, and eighties of the twentieth century, when the current light water reactor technology was developed, the only possible approach to compute the flow inside a fuel bundle was to use one-dimensional sub channel analysis. The sub channel scale could not be resolved. For simulations of the whole reactor core either system codes or homogenization was employed. In system codes resolution of individual assemblies was the state of the art. Homogenization used porous media equations and averaged the thermo hydraulics on reactor core scale. Current potent computing power allows using Computational Fluid Dynamics (CFD) to simulate individual fuel assemblies. Detailed CFD analyses ranging from single subchannels [1, 2, 3] to multiple subchannels [4, 5, 6, 7] and even complete fuel assemblies [8, 9] using different CFD turbulence

modeling techniques, like Reynolds Averaged Navier Stokes (RANS) [1, 2, 3, 6, 8, 9], Large Eddy Simulation (LES) [4, 5, 7] and Direct Numerical Simulation (DNS) [2] have been reported. Yet the large number of fuel assemblies within the core forbids exploiting such detailed CFD simulations for core wide or even in most cases fuel assembly wide simulation.

In order to profit from the fast development of commercial CFD software, new approaches of applying CFD to fuel bundles are assessed by different teams. This paper will describe the approaches used by NRG in the Netherlands and KIT in Germany. Both approaches are based on resolving the geometry of the fuel assembly to a certain degree. However, the resolution of the employed meshes is much lower than in the traditional detailed CFD analyses. Therefore, the approaches are called Low Resolution Geometry Resolving (LRGR) CFD and Coarse-Grid-CFD (CGCFD). No new models have been added to existing CFD codes and the approaches in fact just use the existing possibilities of the employed codes. Therefore, the described developments are referred to as approaches, rather than new models. These approaches are based on low resolution meshes and can be applied with and without a sub grid model (SGM) as will be explained below.

This paper will describe the newly developed LRGR and CGCFD approaches with and without SGM in section 1. Section 2 explains how the grid resolution of the low resolution meshes was selected. Some applications of both the LRGR CFD and the CGCFD approach, with and without SGM will be discussed in section 3. Finally, section 4 will present the conclusions.

1. Low Resolution Mesh Approaches

As explained in the introduction, the approaches seek to profit from the fast development of commercial CFD software and are developed independently by NRG in the Netherlands and KIT in Germany. The two approaches are similar in their use of low resolution grids meanwhile maintaining the important geometrical features. However, they differ in the way the flow physics are taken into account. Within NRG, the approach has been directed towards LRGR CFD without any model for the non-resolved sub grid physics, whereas at KIT, for the CGCFD approach sub grid models are used to involve these particular flow physics.

A similar approach was recently reported by researchers from Argonne National Lab in the USA [10]. They try to fill the gap between the detailed CFD approaches and the traditional subchannel approach by proposing an intermediate-resolution modeling approach. Their objective is to develop scalable intermediate-resolution assembly modeling methods in which the anisotropic flow behavior is resolved, to support full-core transient modeling coupled to existing or emerging neutronics and fuel performance models. In fact, they examined two ways to reduce the number of computational volumes compared to their detailed simulations reported in [6] and [7]. The first way is use a spiral fin to replace the wire wrap. The second way is to simulate a bare rod bundle and introduce a momentum source term that spirals around each rod. In fact, these two ways are similar to the LRGR approaches without and with SGM from the authors as described below.

1.1 LRGR approach without SGM

At NRG, in order to bridge the gap between traditional fuel assembly simulation approaches using system codes, subchannel codes or porous medium approaches and the detailed CFD approaches to analyze single sub-channels, an LRGR CFD approach is applied. This approach does not take into account the physics which is included at scales with resolution lower than the mesh resolution. Therefore, this approach will be denoted as LRGR CFD without Sub Grid Model (SGM). This

LRGR CFD approach without SGM allows capturing 'medium scale' flow features such as large scale recirculation zones (e.g. behind fuel assembly blockages), which cannot be captured by the system code, subchannel code and porous media approaches, and can serve e.g. to fine-tune the porous parameters which are important input for a porous medium approach. However, it should be noted that the prediction of detailed flow features such as secondary flows is not feasible.

1.2 CGCFD approach with SGM

At KIT it is proposed to combine ideas of sub channel analysis and CFD and develop an approach which takes advantage of the fast development of commercial CFD software and the efficiency of sub channel analysis [11].

The motivation for this approach was the fact, that due to computational restraints it is not possible to simulate a complete rod bundle or a complete reactor core with state of the art CFD software and computational power. In such large cases, code coupling of CFD to subchannel codes is needed. The subchannel codes use semi-empiric correlations and specific model constants that have to be adjusted or adapted for each new case or geometry. The goal of the CGCFD approach is to provide an approach that is as efficient as subchannel codes and becomes independent from experimental or empirical data. Furthermore, advantage should be taken of desirable features of modern CFD solvers, i.e. reliability, robustness and graphical user interfaces. The aim of the CGCFD approach is to compute very large and complex geometries that cannot be tackled with a 'traditional' CFD approach due to need for exceedingly large computational resources. In contrast to subchannel analysis the CGCFD technique can be adopted to many applications beyond the typical subchannel geometry. In [12] this methodology was first applied to simulate a wire-wrap fuel bundle of the High Performance Light Water Reactor (HPLWR) [13]. Computations using an inviscid Euler solver on an extremely coarse grid were tuned to predict the true thermohydraulics by adding volumetric forces. These forces represent the non-resolved sub-grid physics. The volumetric forces cannot be measured directly. However, they can be accessed from detailed CFD simulations resolving all relevant physics. Parameterization of these subgrid forces can be realized analogous to models in sub channel codes.

1.2.1 Methodology of the CGCFD

The CGCFD method applies to problems where similar flow situations repeat frequently in a large domain. Instead of simulating the whole domain with many similar flow patterns at distinct locations, the appearing flow patterns are computed just a single time. The global flow is simulated by assembling local behavior. Such a method works best if the geometry can be subdivided into representative small blocks. Figure 1 describes the general approach of a CGCFD simulation. The first step is the identification of a representative block of the geometry. This step requires physical knowledge on the flow since the selection of the representative block has major impact on the results of the CGCFD. In the next two steps detailed CFD simulation of the representative block are performed including parametric studies for potential flow conditions. From the detailed CFD simulations volumetric forces are extracted which represent the most important input for the CGCFD. Note that a very careful detailed CFD must be performed since all inaccuracies will directly enter the CGCFD results. Details on the derivation of the volumetric forces are explained in chapter 1.2.2. Since a frictionless Euler solver without turbulence model is used to perform the CGCFD effects of turbulence and friction are completely embedded in the volumetric forces. The next step is parameterization of the volumetric force terms with relevant flow conditions. Here we can take advantage of subchannel analysis which suggests a robust parameterization for CGCFD of fuel assemblies. In the last two steps the coarse mesh of the complete geometry is setup and the Euler equations with implemented volumetric force terms are solved.

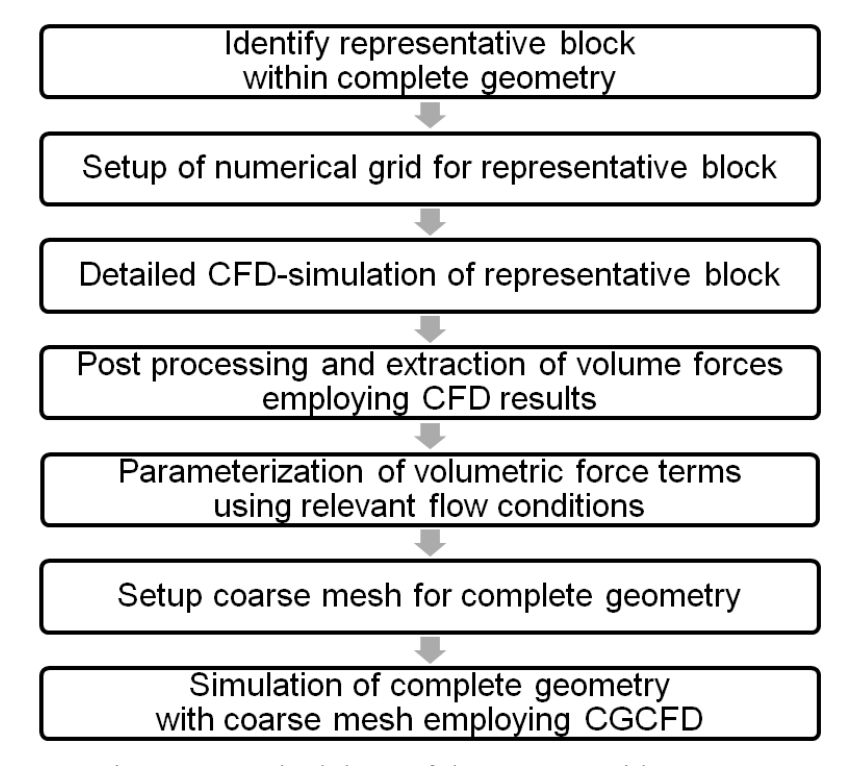


Figure 1 Methodology of the Coarse-Grid-CFD

1.2.2 Theoretical background: Derivation of the sub-grid source terms

In system codes or sub channel analysis the conservation equations are integrated over rather large control volumes and models are used for friction losses and transport between neighboring channels. When using CGCFD the required terms can be evaluated directly from fully resolved fields. Stoke's integration of the steady-state viscous momentum equation (1) reads:

$$\nabla \cdot (\rho \vec{v} \otimes \vec{v}) = -\nabla \operatorname{Ip} + \nabla \cdot \sigma , \qquad (1)$$

$$\oint_{\mathcal{O}} (\rho \vec{v} \otimes \vec{v}) \cdot \vec{n} \cdot dO = - \oint_{\mathcal{O}} (lp) \cdot \vec{n} \cdot dO + \oint_{\mathcal{O}} (\sigma) \cdot \vec{n} \cdot dO$$
(2)

In the CGCFD the Euler equations (3) are extended by an additional volumetric force term $\vec{\mathbf{F}}$ which replaces the nonresolved terms. Upon Stoke's integration we find

$$\nabla \cdot (\rho \vec{v} \otimes \vec{v}) = -\nabla \operatorname{Ip} + \vec{F}, \tag{3}$$

$$\oint_{O} (\rho \vec{v} \otimes \vec{v}) \cdot \vec{n} \cdot dO = - \oint_{O} (lp) \cdot \vec{n} \cdot dO + \iiint_{V} \vec{F} \cdot dV$$
(4)

If the coarse resolution is chosen such that the convective fluxes are reasonably resolved, equations (2) and (4) are consistent. The force term \vec{F} replacing the non-resolved viscous terms can be evaluated as,

$$\iiint_{V} \vec{F} \cdot dV = \oint_{O} (\sigma) \cdot \vec{n} \cdot dO$$
 (5)

Note that these forces include turbulence and non-resolved form losses. In general the fully resolved fields are not available. In fuel assembly simulation, typically the same geometry with near identical flow patterns repeats all over the core region. Therefore, the detailed simulation can be computed for a generic representative small section and possible variations can be tabulated or parameterized.

2. Low Resolution Meshes

2.1 Low Resolution Meshes for LRGR CFD without SGM

Typically a detailed flow analysis in a single sub channel of a fuel assembly requires a mesh resolution of 1 million computational cells, see e.g. [1]. A representative fuel assembly normally employs about 200 to 400 such sub channels. Thus, nowadays a detailed simulation of an entire fuel assembly is very challenging or only feasible with extremely large computational power. Therefore, it is important to determine a suitable computational grid, that has appropriate convergence capabilities and sufficiently captures the main flow features and thereby the temperature.

Simulations are carried out on a single sub-channel of a square fuel. A Reynolds Averaged Navier-Stokes (RANS) based turbulence model is used. For the current low resolution grid analyses the SST k- ω turbulence model is employed in combination with wall functions. Although higher order models and anisotropic models are usually applied for detailed CFD analyses, such models will not lead to improved results with the employed low resolution grids. A constant uniform flow velocity of 1.5 m/s is used at the inlet, a zero static pressure at the outlet and specified heat fluxes are applied on the walls. Lead is used as the working fluid with temperature dependent properties from the OECD handbook [14].

Figure 2 shows the cross-sectional mesh for the reference grid and two low resolution grids used in the grid resolution study. This figure also shows the lead temperature at the outlet for different grids. Analysis of the velocity and vorticity fields demonstrated that the grid coarsening has a strong influence on the analyzed flow field. Relative to the cross-flow seen in the reference grid, the lowest resolution grid (number 5) does not capture any secondary flow (cross-flow) at all. However, from figure 2 it can be qualitatively observed that lower resolution grids do not have a remarkable effect on the analyzed temperature field relative to the velocity field. This is probably due to the fact the main mechanism for heat transport is dominated by the axial flow. The well known secondary flows which are subject of many detailed CFD analyses have a limited influence on the heat transport. Nuclear reactor designers are mostly interested in the temperature field and pressure drop. In the reported analyses, the main focus has been the temperature field. Therefore, it is proposed to neglect the deficiencies clearly detected in the less resolved flow field and to work with approximated flow fields.

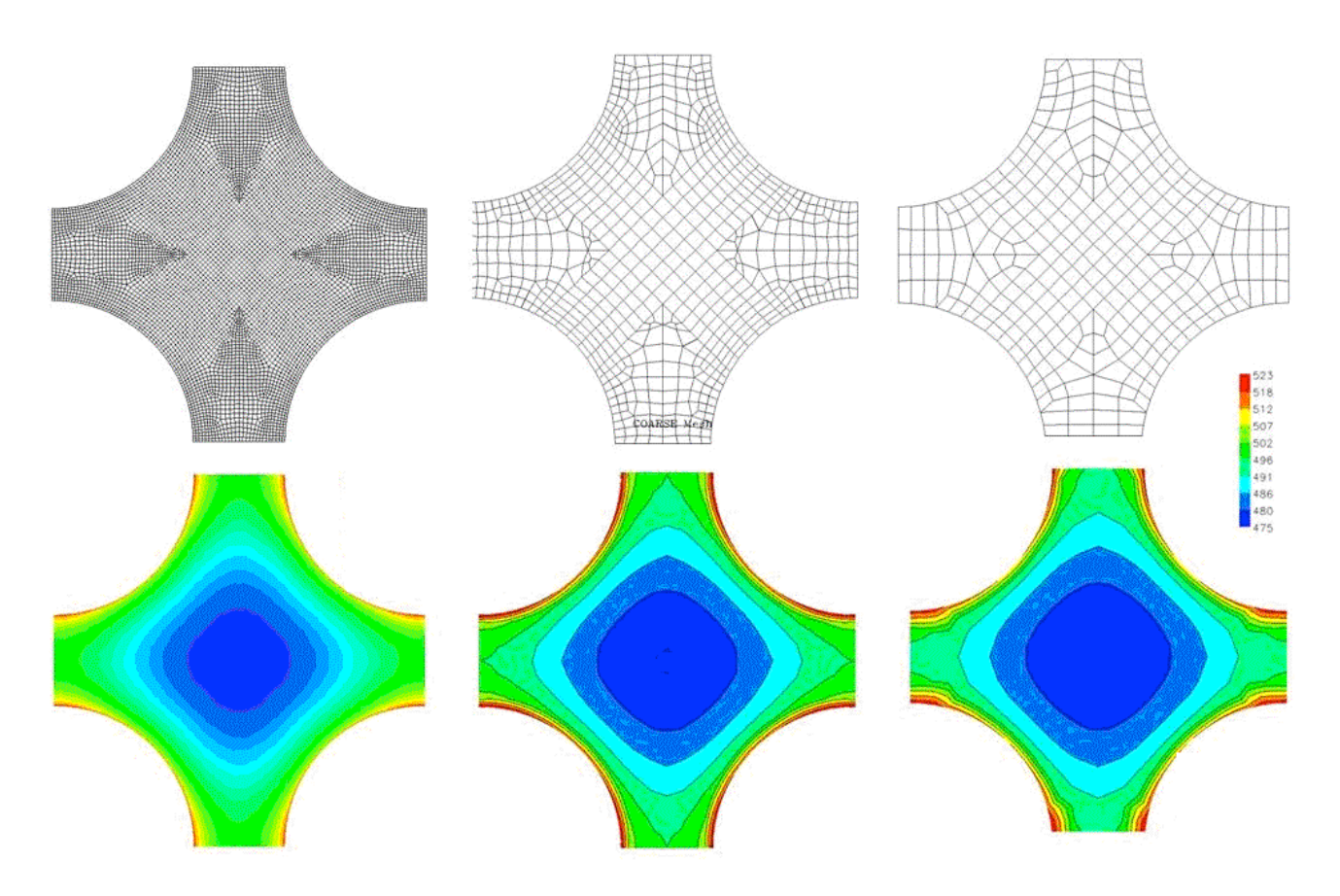


Figure 2 Meshes and temperature distributions for 3 employed grids (Reference, Grid 1, and Grid 5)

Table 1 Grid specifications and accuracy of results

Grid	No. of Elements	Maximum y+	Max. Temperature (T_max in °C)	% Relative Error with respect to temperature rise
Reference	1.1 Million	42	519.2	0
Grid 1	37000	133	523.71	10.0
Grid 2	19000	133	523.45	9.4
Grid 3	21000	168	521.27	4.6
Grid 4	11000	168	521.37	4.8
Grid 5	9500	300	525.85	14.8

Table 1 summarizes the different grids that are used in this grid resolution study, including the y+values which provide an indication of the wall treatment and their effect on the maximum temperature at the outlet of the sub-channel. The relative error in temperature is defined as:

Relative Error =
$$\frac{\left(T_{\text{max_grid}} - T_{\text{max_ref}} \right)}{T_{\text{max_ref}} - T_{\text{min_ref}}}$$
Outlet

Here, temperatures (*T*) are considered at the outlet of a sub-channel at which their corresponding maxima occurs. The subscript *max_grid* means the calculated maxima with different grids, *max_ref* means the calculated maximum for the reference fine grid and *min_ref* means the calculated minimum value for the reference grid. These values are provided in table 1.

From the percentage relative error in the RANS based time mean temperatures with respect to the reference grid it is concluded that all grids show a sufficiently accurate temperature field. Even the lowest resolution grid with 9500 elements may be used for simulation of an entire fuel assembly with sufficient accuracy to study the effects of blockages. Furthermore, it should be noted that the low resolution grids all show over predictions of the maximum temperatures. This will lead to conservative results with respect to the calculated coolant and cladding temperatures.

2.2 Low Resolution Meshes for CGCFD with SGM

In the assessment of a quadratic wire-wrap fuel assembly [12] (figure 3A), it is shown that the grid resolution should be chosen such that at least five control volumes cover each sub channel. The center cell contains most of the axial flow, while the transverse transport between neighboring sub channels is concentrated in the four surrounding cells. A closer look to the set up and results of the HPLWR rod bundle CGCFD can be found in [12].

The same strategy is employed for a hexagonal assembly where now a wedge central cell surrounded by three hexahedral cells represents each sub channel as shown in figure 3B. The spacer (figure 4A) subdivides the flow into separate flow domains. In the low resolution simulation these details are ignored and the separate flow domains are combined. The flow obstruction of the spacers is modeled in the coarse mesh by slightly deforming the rods (figure 4B black). Note that the flow domain volume and flow cross sections are preserved. The coarse modeling of the CGCFD results in only about 30000 computational cells for a simulation of a complete rod bundle. The coarse meshing makes it possible to simulate a complete reactor core with state of the art computational power. More detailed information can be found in [11] and [21].

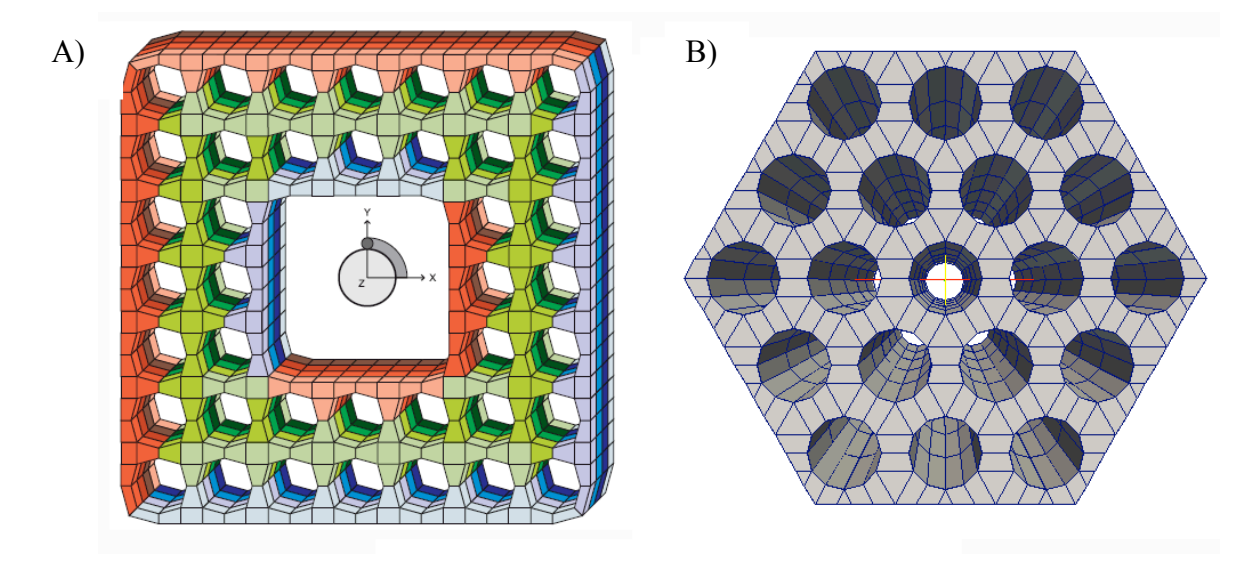


Figure 3 Employed meshes for square (A) and hexagonal fuel assembly arrangement (B)

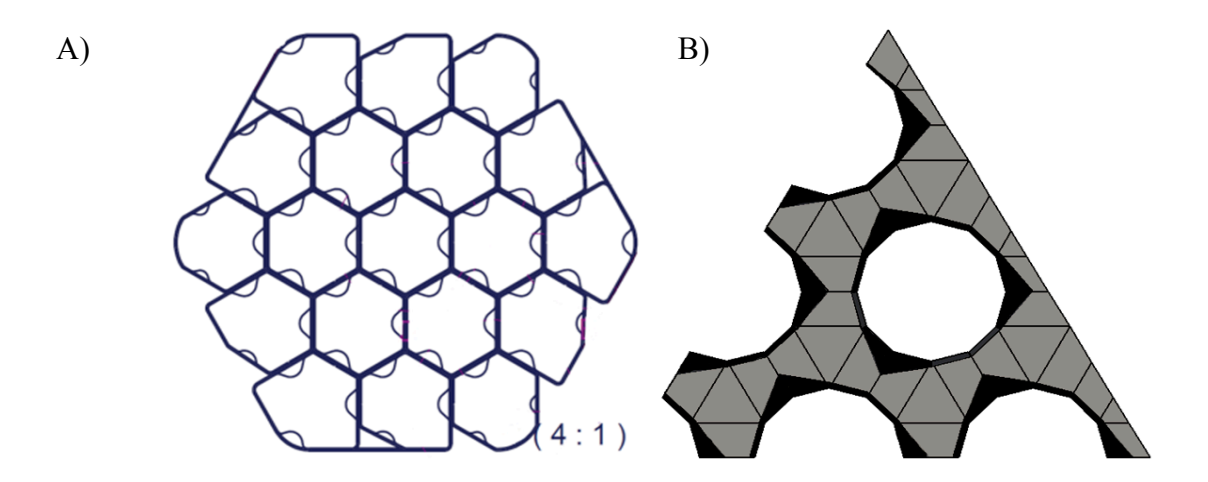


Figure 4 Spacer region: (A) Blueprint spacer (B) Obstruction due to spacer grid in CGCFD (black)

3. Applications

3.1 Application of LRGR CFD without SGM

The LRGR CFD approach without SGM has been applied to determine the effects of complete and partial blockage of a fuel assembly in the ELSY lead cooled reactor design [15]. Although validation was only performed for a subchannels without blockage, it is assumed that the conclusions will also be valid for blocked assemblies. For the ELSY reactor, two different core geometries were under consideration. The reference core design consisted of open square fuel assemblies, whereas the alternative design envisaged a more traditional closed hexagonal fuel assembly design. One of the assumptions for preferring the open square fuel assembly design was based on the possibility of inter fuel assembly mixing in case of a fuel assembly blockage. For that reason, a complete inlet blockage scenario of the open square fuel assembly design was studied using the LRGR approach without SGM. On the other hand, for the closed hexagonal fuel assembly design, analyses of partial inlet and internal blockage were requested. Also these were assessed using the LRGR approach without SGM.

The SST k-ω turbulence model is employed in combination with wall functions. A constant uniform flow velocity of 1.9 m/s and temperature of 400°C is used at the inlet, a zero static pressure at the outlet and specified uniform heat fluxes are applied on the walls of the fuel rods. Lead is used as the working fluid with temperature dependent properties from the OECD handbook [14].

Figure 3 shows the geometry and the computational grid employed for the closed hexagonal ELSY fuel assembly. Inlet blockages up to 16 % were assumed. Furthermore, an internal blockage is modeled, in which 40 % of the height of the fuel assembly around the center and 60 % of the cross-sectional area around the central fuel pin is blocked. This case resembles a blockage which has occurred in the sodium cooled KNK2 reactor in Karlsruhe by corrosion particles within the coolant flow which got caught on a fuel rod surface [16]. Thus, a blockage layer grows affecting the flow throughput and the heat conduction. In the present simulations, heat conduction within the fuel rod is not considered, thus we assume that the blockage material has infinite conductivity, meaning that the blockage has the same mean rod power as the fuel rods.

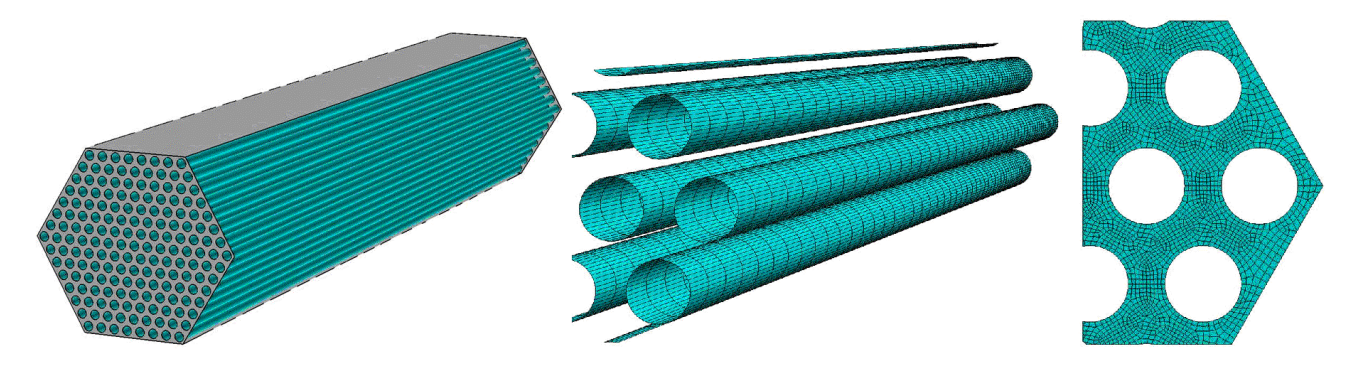


Figure 5 Computational geometry and grid of the closed hexagonal ELSY fuel assembly.

The analyses showed that a partial blockage of a closed hexagonal fuel assembly design at the inlet of up to 16 % cross section (see figure 6) and internally, leads to an average temperature increase at the assembly outlet of only \sim 2 °C. Thus, detection of blockages at the outlet header of each single fuel assembly will strongly depend on the mixing in the outlet header. The maximum cladding temperature observed is \sim 673 °C, so failure of fuel cladding will not occur.

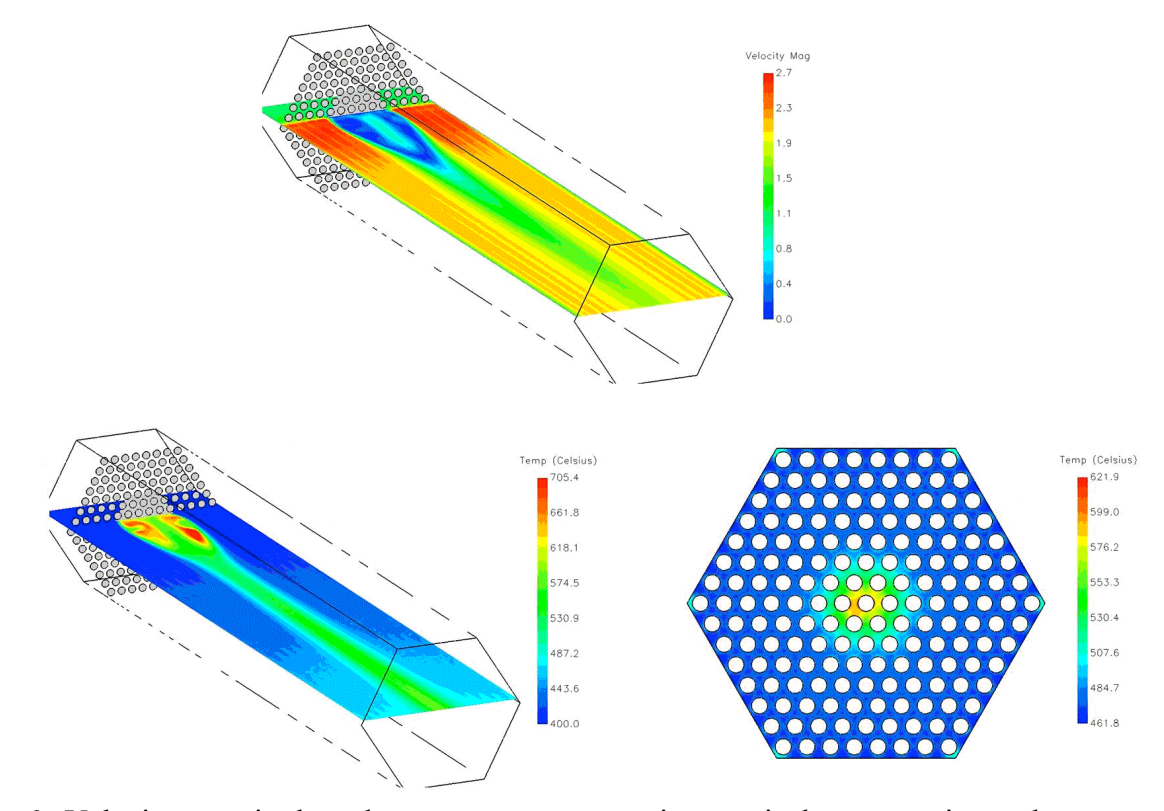


Figure 6 Velocity magnitude and temperature contours in a vertical cross-section and temperature at the outlet of the closed hexagonal ELSY fuel assembly for 16 % inlet blockage.

Consequences of a complete inlet blockage of the open square ELSY fuel assembly were also analyzed with the LRGR CFD approach without SGM. Figure 7 shows the selected computational domain which

includes an area of four fuel assemblies. This figure also reveals the employed grid for the analyses.

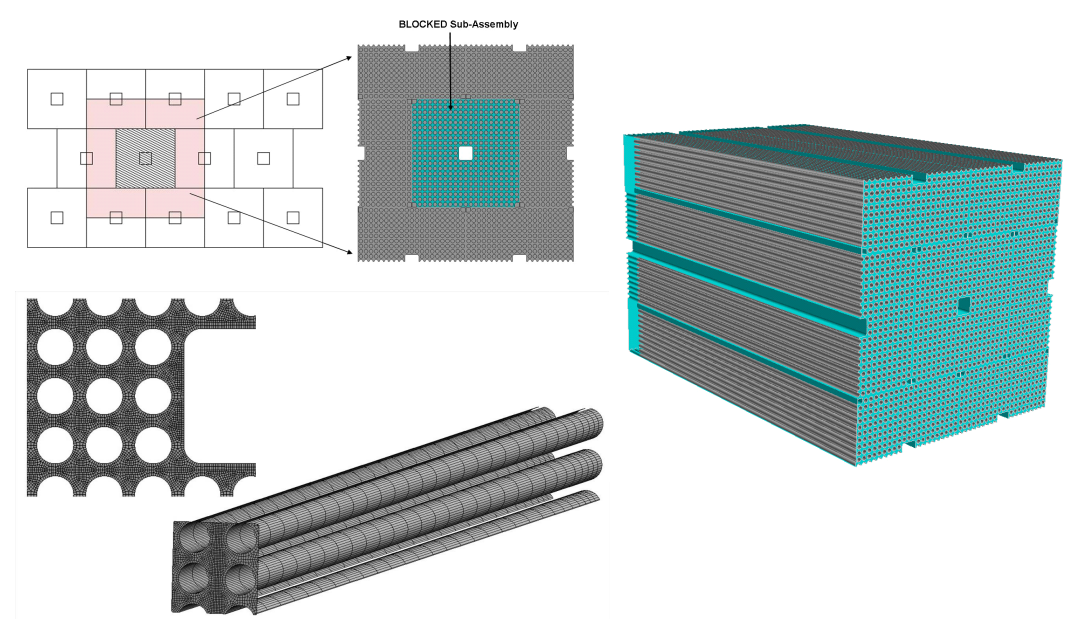


Figure 7 Computational domain and grid of the square open ELSY fuel assembly

Figure 8 shows the axial velocity and temperature contours in a vertical cross section. It is clear that behind the blockage, a huge recirculation zone occurs. Furthermore, this result reveals that, in contrast to what was often assumed, there is limited mixing from neighboring fuel assemblies.

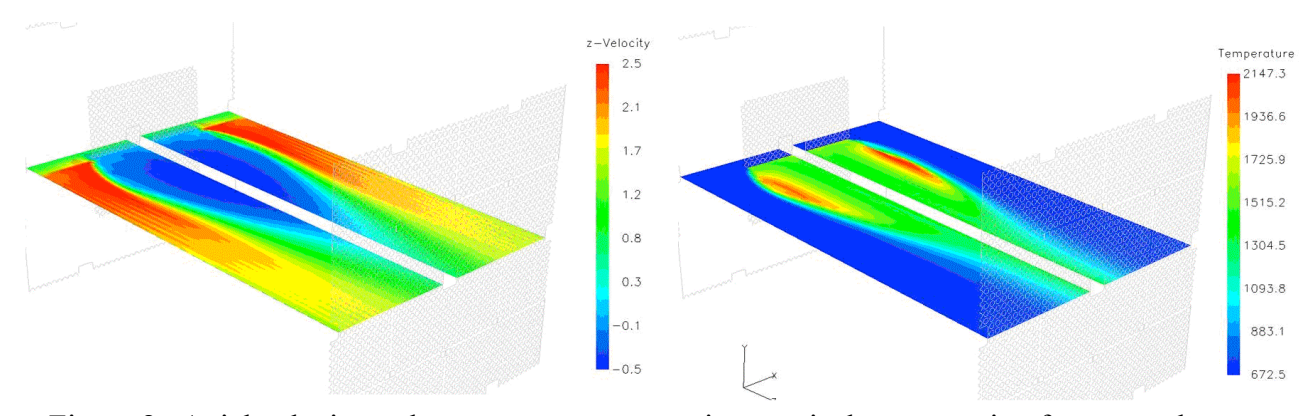


Figure 8 Axial velocity and temperature contours in a vertical cross-section for a complete open square ELSY fuel assembly blockage

Figure 9 shows the temperatures occurring just behind the blockage in the horizontal plane where the highest temperatures have been deducted from the LRGR CFD analysis and at the outlet plane. These results reveal that under the assumed conditions failure of fuel cladding will occur. If there is a possibility to measure temperatures at the outlet of individual subassemblies with high precision, then an early detection of a total inlet blockage for the open square fuel assembly design might be possible. However, most probably fuel pin failure has already occurred when coolant outlet temperatures increase by a detectable amount. A time dependent simulation of consequences of an inlet blockage increasing with time would become necessary to evaluate detection capabilities of massive inlet blockages by a single average coolant outlet temperature measurement at each subassembly without entering into massive fuel pin failures. These were out of the scope for the present work. The analyses are described in detail in [17] and [18].

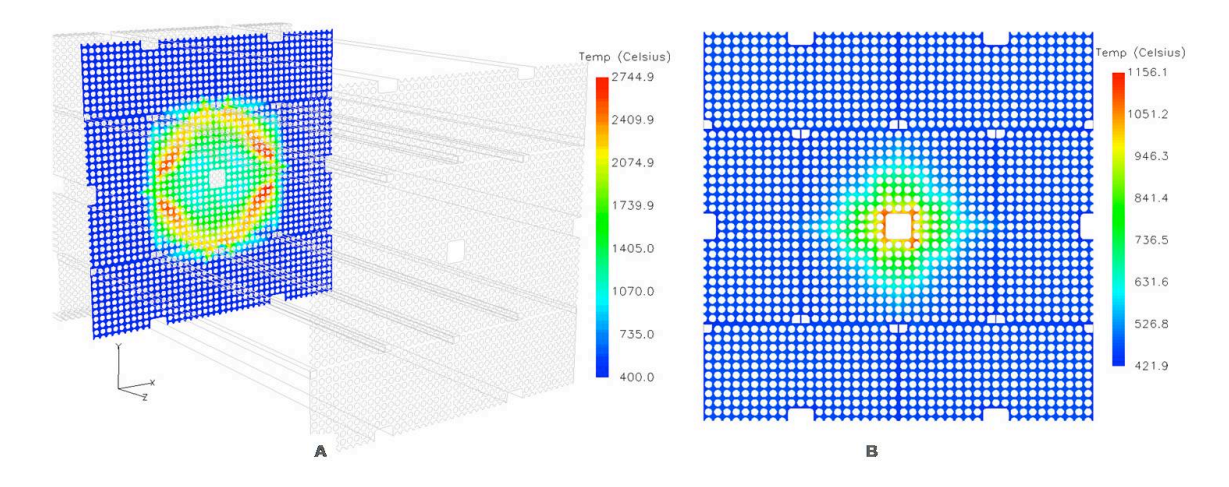


Figure 9 (A) Cross-sectional plane just behind the blockage indicating the highest temperatures and (B) temperature contours at the outlet

3.2 Application of CGCFD with SGM

The CGCFD approach with SGM is applied to the experiments performed at the KALLA laboratory in Karlsruhe [19]. Detailed CFD simulations were performed [20] in order to predict the pressure drops occurring in the experimental 19 pin water cooled rod bundle. These simulations which approach was verified to first experimental results, served now as reference for the CGCFD simulation. The detailed simulations were performed with Star-CCM using the high-Reynolds-number k-\varepsilon turbulence model. The k-\varepsilon turbulence model was chosen since the pressure drop in the selected rod bundle geometry primarily is due to form losses, see [20] and [22]. In bare subchannels, secondary flow may lead to additional friction that cannot be described with the isotropic k-\varepsilon turbulence model. However, in the considered bundle form losses dominate over the friction losses allowing for the use of isotropic models at reasonable accuracy. Moreover for the purpose of demonstrating the Coarse-Grid-CFD consistency between the two numerical methods is more important than the very best accuracy of the reference simulation.

The numerical setup and the flow conditions for the CGCFD are shown in figure 10 and at the top of figure 11.

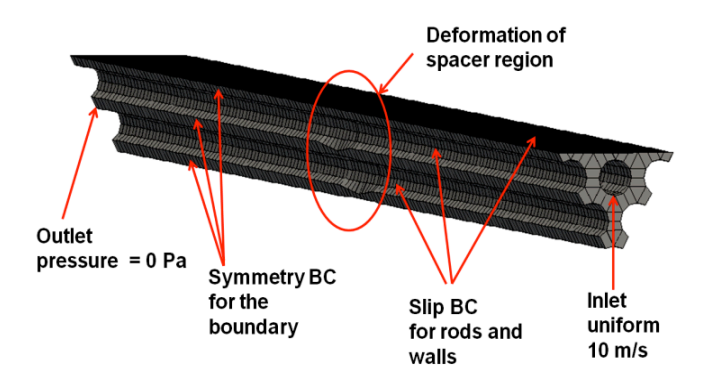


Figure 10 Mesh showing deformation of rods in spacer region and boundary conditions

The CGCFD simulation runs three orders of magnitude faster than the detailed simulation. Moreover, it requires much smaller computational resources. Figure 11 (A) depicts the results of the detailed CFD simulation of the water rod bundle experiments. In the picture the pressure is plotted along four axial lines through the rod bundle. In the rod bundle cross section inset of figure 11 and 12 these line positions are marked with green dots labeled L1-L4. Picture 11 (B) shows the results of the CGCFD of the water rod bundle experiment. In figure 12 (A) and 12 (B) the pressure along the four axial lines through the spacer for the detailed CFD simulation is compared to the pressure of the CGCFD.

The frictional losses along the rods, pressure drop due to acceleration in the spacer region, and pressure recovery are reproduced on the coarse grid. Note, that in order to get these results the forces in the spacer had to be adjusted to account for additional flow obstruction by the boundary layers on the spacer. More details can be found in [11] and in [21].

	Solver	Inflow	Turbulence model	Number of cells	CPU-Time
	Detailed CFD	U= 10 m/s	Κ-ε	500000	Ca. 30 h
	CGCFD	U= 10 m/s	-	4884	Ca. 5 min
90 80 70 60 50		Line 1 detailed Line 2 detailed Line 3 detailed Line 4 detailed	90 80 70 60 8 50	-⊒-Line Line	1 coarse 2 coarse 3 coarse 4 coarse

Length in [m]

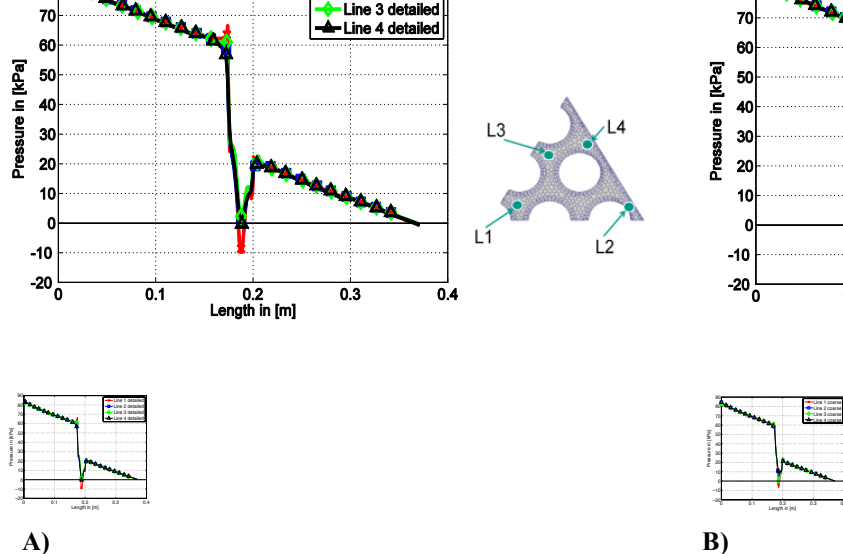


Figure 11: Pressure losses in hexagonal rod bundle

- A) detailed CFD
- B) Coarse-Grid-CFD

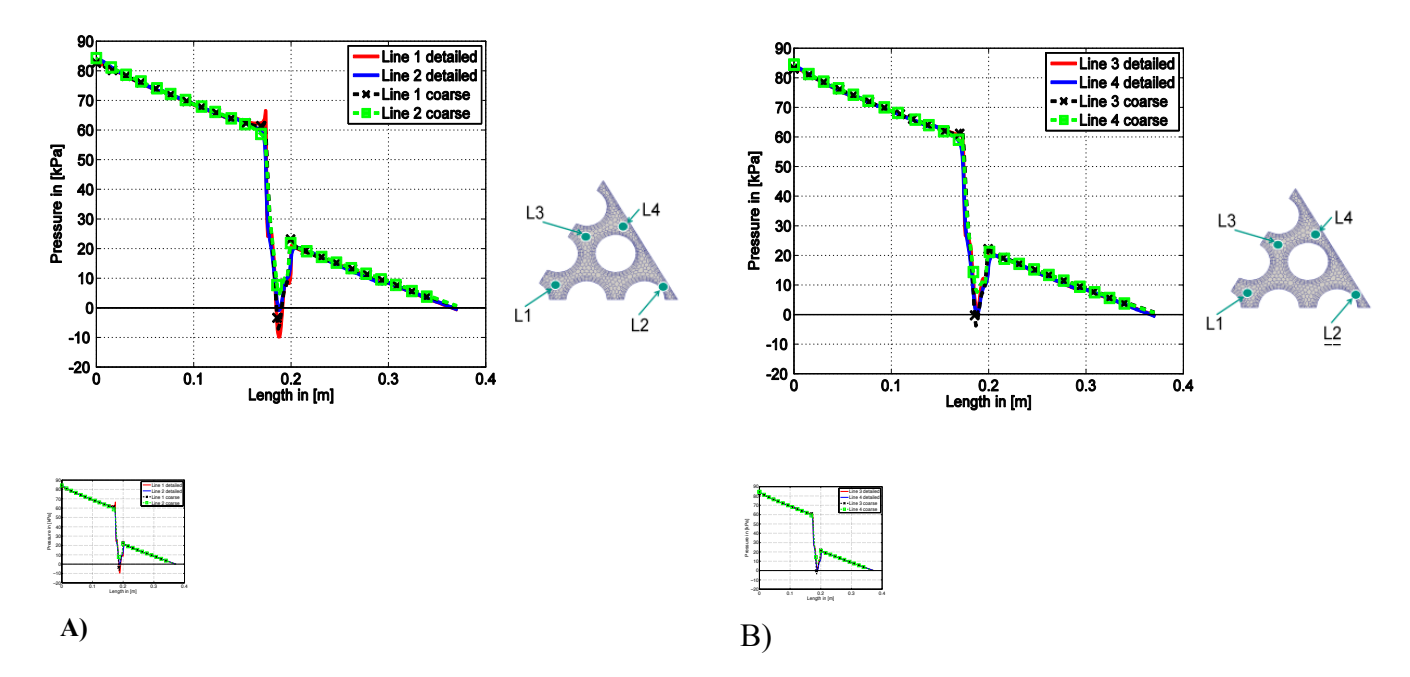


Figure 12: Pressure loss in hexagonal rod bundle (u_{inlet} =10 m/s): Comparison of detailed CFD (detailed) and Coarse-Grid-CFD (coarse)

- A) Line 1 and Line 2
- B) Line 3 and Line 4

4. Conclusions

In order to profit from the fast development of commercial CFD software, new approaches of applying CFD to fuel bundles are developed by different teams. This paper presented and described the new approaches.

Both approaches use coarse meshes whose resolution is much lower than state of the art resolution for a detailed CFD simulation. Therefore the method which is developed at the NRG is called the Low Resolution Geometry Resolving (LRGR) CFD and the method that is developed at the KIT is called Coarse-Grid-CFD. Both approaches don't use new models or codes. They rather use the possibilities of existing, state of the art CFD codes. Therefore, the described developments are referred to as new approaches, rather than new models. Such LRGR approaches can be applied with (CGCFD) and without a sub grid model (LRGR)

Table 2 summarizes the existing CFD approaches, ranging from detailed CFD to LRGR CFD without SGM which serves to fill the gap between detailed CFD and traditional subchannel approaches, and to CGCFD with SGM which basically uses the modern solver techniques available in CFD as an alternative to the traditional subchannel approaches.

Table 2 Summary of the LRGR CFD approaches with and without SGM

Table 2 Sammary					
Approach	Detailed CFD	LRGR CFD	CGCFD		
		without SGM	with SGM		
Mesh					
Solve	All (Flow, bulk turbulence, boundary layers, secondary flows)	Main flow characteristics Bulk turbulence	Main flow characteristics		
Sub Grid Model			All		
Application	Part of a fuel assembly	Complete fuel assembly	Complete core		

5. Acknowledgements

Parts of the work described in this paper by the authors were carried out in the frame of and supported by the FP6 EC Integrated Project ELSY No. FI6W-036439, by the FP6 EC HPLWR Phase 2 project FI6O-036230, and by the FP7 EC Collaborative Project THINS No. 249337.

6. References

- [1] Chandra L., Roelofs F., Houkema M., Jonker B., 2009. A Stepwise Development and Validation of a RANS based CFD Modelling Approach for the Hydraulic and Thermalhydraulic Analyses of Liquid Metal Flow in a Fuel Assembly. Nuclear Engineering & Design, vol. 239, p.p. 1988-2003.
- [2] Baglietto E., Ninokata H., Misawa T., 2006. CFD and DNS Methodologies Development for Fuel Bundle Simulations. Nuclear Engineering & Design, vol. 236, p.p. 1503-1510.
- [3] Chang D., Tavoularis S., 2008. Simulations of Turbulence, Heat Transfer and Mixing Across Narrow Gaps Between Rod-bundle Subchannels. Nuclear Engineering & Design, **vol. 238**, p.p. 109-123.
- [4] Benhamadouche S., Le-Maitre C., 2009. Large Eddy Simulation of the Flow along four Subchannels Downstream a Mixing Grid in a PWR. <u>NURETH13</u>, Kanazawa, Japan.
- [5] Ikeno T., Kajishima T., 2010. Analysis of Dynamical Flow Structure in a Square Arrayed Rod Bundle. Nuclear Engineering & Design, vol. 240, p.p. 305-312.
- [6] Pointer D., Fischer P., Siegel A., Smith J., 2008. RANS-based CFD Simulations of Wire-Wrapped Fast Reactor Fuel Assemblies. <u>ICAPP 2008</u>, Anaheim, USA.
- [7] Fischer P., Lottes J., Siegel A., Palmiotti G., 2007. Large eddy simulation of wire wrapped fuel pins. <u>Joint Int. Topical Meeting on Math. and Comp. And Supercomputing in Nuclear Applications</u>, Monterey, USA.

- [8] Gajapathy R., Velusamy K., Selvaraj P., Chellapandi P., Chetal S., 2009. A Comperative CFD Investigation of Helical Wire-wrapped 7, 19, 37 Fuel Pin Bundles and Its Extendibility to 217 Pin Bundle. Nuclear Engineering & Design, vol. 239, p.p. 2279-2292.
- [9] Péniguel C., Rupp I., Rolfo S., Guillaud M., 2010. Thermal-hydraulics and Conjugate Heat Transfer Calculation in a Wire-wrapped SFR Assembly. <u>ICAPP 2010</u>, San Diego, USA.
- [10] Hu R., Fanning T., 2010. Intermediate-Resolution Method for Thermal-Hydraulics Modeling of a Wire-Wrapped Pin Bundle. Transactions of the American Nuclear Society, **vol. 103**, pp. 1003-1005.
- [11] Class A., Viellieber M., Batta A., 2011. Coarse-Grid-CFD for Pressure Loss Evaluation in Rod Bundles. <u>ICAPP 11</u>, Nice, France.
- [12] Himmel S., 2009. Modellierung des Strömungsverhaltens in einem HPLWR-Brennelement mit Drahtwendelabstandshaltern (in German). PhD Thesis, Institut für Kern- und Energietechnik (KIT), Karlsruhe, Germany.
- [13] Schulenberg T., Starflinger J., Marsault P., Bittermann D., Maraczy C., Laurien E., Lycklama J.A., Anglart H., Andreani M., Ruzickova M., Heikinheimo L., 2009. European Supercritical Water Cooled Reactor. <u>FISA 2009</u>, Prague, Czech Republic.
- [14] OECD/NEA, 2007. Handbook on Lead-bismuth Eutectic Alloy and Lead Properties, Materials Compatibility, Thermal-hydraulics and Technologies. OECD NEA No. 6195, ISBN 978-92-64-99002-9.
- [15] Alemberti A., Carlsson J., Malambu E., Orden A., Cinotti L., Struwe D., Agostini P., Monti S., 2009. European Lead Fast Reactor: ELSY. FISA 2009, Prague, Czech Republic.
- [16] Brockmann K., et al., 1990. Temperature Drift at Outlet Temperature of the KNK II Subassemblies. Int. Fast Reactor Safety Meeting, Snowbard, USA.
- [17] Castelliti D., Arien B., Bandini G., Meloni P., Polidori M., Struwe D., Bubelis E., Schikorr M., Böttcher M., Carlsson J., Gopala V.R., Chandra L., Roelofs F., 2010. Safety analysis of plant accidents representative for design basic conditions. ELSY DEL/10/030, Mol, Belgium.
- [18] Bubelis E., Schikorr M., Bandini G., Meloni P., Polidori M., Mikityuk K., Chandra L., Roelofs F., Carlsson J., 2010. Results of analyses for Design Extension Conditions (DEC). ELSY DEL/10/031, INR2010_003, Karlsruhe, Germany.
- [19] Litfin K., Class A., Daubner M., Gnieser S., Stieglitz R., 2008. Experimental investigation of sub channel flow distribution in a Hexagonal rod bundle experiment. IEMPT10, Mito, Japan.
- [20] Batta A., Class A., Litfin K., Wetzel T., 2010. Numerical Study on Flow Distribution and Turbulent Flow in XT-ADS Rod Bundle Water Experiment. <u>NUTHOS-8</u>, Shanghai, China.
- [21] Class A., Himmel S., Viellieber M., 2011. Coarse-Grid-CFD: An Advantageous Alternative to Subchannel Analysis. <u>Jahrestagung Kerntechnik 2011</u>, Berlin, Germany.
- [22] Litfin K., Batta A., Class A.G., Wetzel T., Stieglitz R., 2009. Flow distribution and turbulent heat transfer in a hexagonal rod bundle experiment. Institut für Kern- und Energietechnik, Karlruhe, Germany.